

Excitation of ^{229}Th nuclei in laser plasma: the energy and half-life of the low-lying isomeric state

P. V. Borisyyuk,^{1,*} E. V. Chubunova,¹ N. N. Kolachevsky,^{2,1}
Yu. Yu. Lebedinskii,¹ O. S. Vasiliev,¹ and E. V. Tkalya^{3,1,4,†}

¹National Research Nuclear University MEPhI, 115409, Kashirskoe shosse 31, Moscow, Russia

²P. N. Lebedev Physical Institute of the Russian Academy of Sciences, 119991, Leninskii prospekt 53, Moscow, Russia

³Skobeltsyn Institute of Nuclear Physics Lomonosov Moscow State University, Leninskie gory, Moscow 119991, Russia

⁴Nuclear Safety Institute of RAS, Bol'shaya Tuskaya 52, Moscow 115191, Russia

(Dated: April 3, 2018)

The results of experimental studies of the low-energy isomeric state in the ^{229}Th nucleus are presented. The work is consisted of several stages. During the first stage ^{229}Th nuclei were excited with the inverse internal conversion to the low-lying isomeric level in plasma that was formed by laser pulse at the ^{229}Th -containing target surface. Then thorium ions having excited nuclei were extracted from the plasma by an external electrical field and implanted into thin SiO_2 film grown on a silicon substrate (that is a dielectric material with about 9 eV band-gap). Gamma decay of isomeric nuclei was registered during the second stage by the general methods of the electron spectroscopy after the photon-electron emission from the silicon substrate. Substitution of the photon registration with the electron one allowed us to increase the desired signal by several orders of magnitude and detect the ^{229}Th nuclei decay. During the third stage the electron spectra from standard Xe VUV source was obtained that allowed determining the energy of photons. In order to prove that the detected signal is caused by isomeric ^{229}Th nuclei decay a series of experiments was carried. The analysis of electron spectra gives the following results: the energy of the nuclear transition is $E_{\text{is}} = 7.1^{(+0.1)}_{(-0.2)}$ eV, the half-life of the isomeric level in bare nucleus in vacuum is $T_{1/2} = 1880 \pm 170$ s, the reduced probability of the isomeric nuclear transition is $B_{\text{W.u.}}(M1; 3/2^+ \rightarrow 5/2^+) = (3.3 \pm 0.3) \times 10^{-2}$.

PACS numbers: 23.20.Lv, 21.10.Tg, 27.90.+b

I. INTRODUCTION

In 1976 Kroger and Reich discovered a low-lying state in ^{229}Th nucleus with the energy $E_{\text{is}} < 100$ eV analyzing γ -radiation after decay of ^{233}U isotope $^{233}\text{U} \rightarrow ^{229}\text{Th} + ^4\text{He}$ [1]. Further experiments carried out by Reich and Helmer in 1990 indicated the extremely low energy of $E_{\text{is}} = 1 \pm 4$ eV for the first excited isomeric state [2]. Four years later the same authors presented an improved value of $E_{\text{is}} = 3.5 \pm 1.0$ eV [3]. However, accurate measurements of γ -transitions in the energy ranges of 29 keV and 42 keV, made in 2007 by Beck *et al.* resulted in significantly different value of $E_{\text{is}} = 7.6 \pm 0.5$ eV [4] (later slightly corrected to 7.8 ± 0.5 eV [5]). The most recent data coming from direct measurements of electron internal conversion process predict that $6.3 \text{ eV} \leq E_{\text{is}} \leq 18.3 \text{ eV}$ [6]. In this work the α decay process of ^{233}U was used for populating the low-lying isomeric state of ^{229}Th which occur with 2% probability [6]. This method sets serious limitations to available experimental configurations because of various decay products, high background and relatively low particle number [6]. Direct excitation of the ^{229}Th isomeric nuclear state would significantly facilitate further research activities, including variety of practical applications, but remains one of the

not yet resolved challenges.

Fundamental interest to this problem is based on a number of unusual physical problems such as electron bridge [7], isomeric state alpha decay [8], photon emission from the nucleus in a dielectric material with a wide bandgap [9, 10], enhancement of the relative effects of the variation of the fine structure constant α and the strong interaction parameter m_q/Λ_{QCD} [11] and others.

As for feasible applications, the main focus is the development of nuclear transition-based laser [12, 13] and highly accurate optical clocks [14–19]. One of the approaches to nuclear transition-based optical clocks is to laser cool a cloud of ^{229}Th ions loaded in a Paul trap [20–22]. Similar approach was developed for trapping $^{229}\text{Th}^{3+}$ Coulomb ion crystals, the first successful trapping of 10^4 ions was reported in [23]. In these experiments electronic transitions with energies near 7.8 eV in trapped thorium ions were carefully measured by laser spectroscopy. The uncertainty budget of proposed ^{229}Th optical clocks was analyzed in [17]. Taking into account the Zeeman and Stark shifts, the Doppler effect, black body radiation shift, and ion micromotion, the relative frequency uncertainty was estimated as $< 10^{-19}$. This is significantly lower than for the best known state-of-the-art optical clocks based on electronic transitions [24].

One of the approaches to directly excite the low-lying isomeric state with photons was developed by Jeet and co-authors [25], and by Stellmer and co-authors [26]. ^{229}Th ions were implanted in transparent crystals like LiCaAlF_6 , LiSrAlF_6 , CaF_2 and other samples [27–30])

*Electronic address: pvborisyuk@mephi.ru (experiment)

†Electronic address: tkalya@srd.sinp.msu.ru (theory)

and then illuminated by intensive VUV (vacuum ultra violet) radiation. These experiments did not succeed in excitation of the isomeric state. One of the feasible reasons could be extremely broad energy range (of approximately one eV or 250 THz) needed to scan in search for the resonance. For any optical method like synchrotron radiation spectroscopy or laser spectroscopy it will require incredibly long time to cover this spectral range, taking into account a narrow expected resonance line width.

We study excitation of ^{229}Th nuclei by inverse internal conversion process in laser plasma which was suggested in [7]. The inverse internal conversion process (IIC [31]) was discussed for the first time by Goldanskii and Namiot in [32] and analyzed in details in the later work [33]. After ablation of ^{229}Th target, ions can be implanted into a wide-gap dielectric material (SiO_2) to prevent electronic internal conversion process which reduces the lifetime of the nuclear isomeric state [9, 10]. Combination of these two methods (plasma formation and ion implantation) allow to directly excite nuclear isomeric state and measure its energy and the lifetime.

II. EXCITATION ^{229}Th NUCLEI IN LASER PLASMA

Laser ablation from ^{229}Th -containing target is one of the methods to directly excite isomeric nuclear state. Theoretical and experimental studies show (see in [33] and references therein) that the inverse internal conversion process is the most efficient for nuclei excitation in the case of ^{229}Th . Plasma electrons of the continuous spectrum with energies \mathcal{E} contribute to IIC process and occupy the ion states of discrete spectrum with energies \mathcal{E}_f . The nucleus in this case is excited by a virtual photon (see in Fig. 1). The considered process is inverse to the isomeric nuclear state decay via internal electron conversion. IIC cross-section for completely vacant ion shell is calculated using the conventional methods of the perturbation theory of quantum electrodynamics [33]

$$\sigma_{\text{IIC}}(\mathcal{E} \rightarrow \mathcal{E}_f) \simeq \delta(E_{\text{is}} - \mathcal{E} + \mathcal{E}_f) \frac{\lambda_e^2}{4} \Gamma_{\text{IC}}(E_{\text{is}}, f) g, \quad (1)$$

where δ is the Dirac delta-function, E_{is} is the energy of the nuclear isomeric state, $\Gamma_{\text{IC}}(\omega_N, f)$ is a partial internal conversion (IC) width of isomeric state for the decay via f ion shell, λ_e is the de Broglie wavelength of plasma electron, $g = (2J_F + 1)/(2J_I + 1)$, and $J_{I,F}$ are the nuclear spins in initial (I) and final (F) states.

Excitation is caused by electrons in the plasma spectrum with energies \mathcal{E}_{res} approaching (within the width Γ_{IC}) the difference of the nuclear transition energy ω_N and the binding energy $|\mathcal{E}_f|$ of the occupying atomic shell. I.e. the process has a pronounced resonance character. The IIC process is most efficient at the electron plasma temperature kT comparable to $\hbar\omega_N$ (in our case $kT \simeq \hbar\omega_N = E_{\text{is}}$). At such temperatures, first, the atomic shells contributing to IIC are ionized, and second,

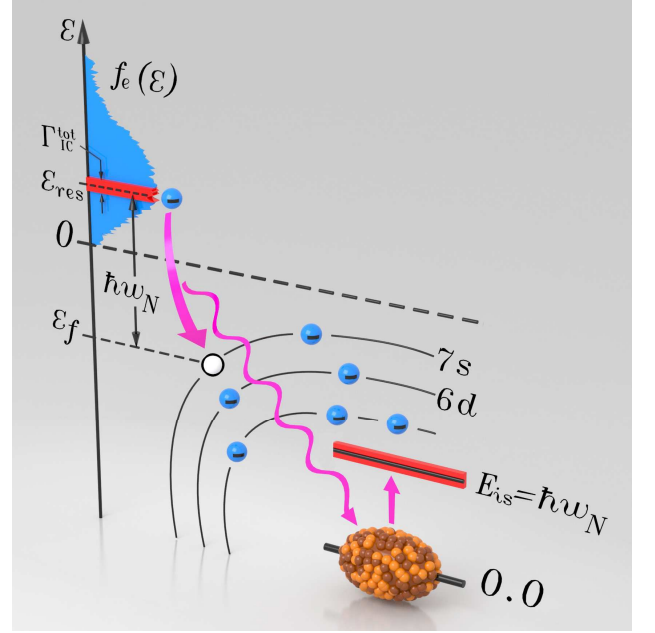


Figure 1: Excitation of ^{229}Th nucleus via inverse internal conversion to the $7s$ electron shell.

the electron density with the energies around $\hbar\omega_N$ is high enough. To reach temperature corresponding to the energy of ≈ 10 eV, a moderate laser intensity of $I \sim 10^{10}$ W cm^{-2} is required [34].

The probability to excite isomeric state in plasma with electron density n_e and electronic energy distribution function $f_e(\mathcal{E})$ is given by [33]

$$\eta_{\text{IIC}} = \int_0^\infty \sigma_{\text{IIC}}(\mathcal{E} \rightarrow \mathcal{E}_f) n_e f_e(\mathcal{E}) \tau v_e \frac{d\mathcal{E}}{kT}, \quad (2)$$

where $v_e = \sqrt{2\mathcal{E}/mc^2}$ is electron velocity (m is the electron mass), and τ is a duration of excitation process or typical laser plasma life time.

After integration the delta function on energy from σ_{IIC} is eliminated. Then the probability can be evaluated as

$$\eta_{\text{IIC}} \simeq \sigma_{\text{IIC}}^{\text{eff}} f_e(\mathcal{E}_{\text{res}}) n_e \tau v_e^{\text{res}}, \quad (3)$$

where

$$\sigma_{\text{IIC}}^{\text{eff}} = \left(\frac{\lambda_e^{\text{res}}}{2} \right)^2 \frac{\Gamma_{\text{IC}}^{\text{tot}}}{kT} \simeq 2 \times 10^{-25} \text{ cm}^2 \quad (4)$$

is the effective cross-section, $\Gamma_{\text{IC}}^{\text{tot}} \simeq 3 \times 10^{-10}$ eV is the total IC width of the nuclear level [this preliminary estimate for the conversion width follows from the middle value of the reduced probability of the nuclear isomeric transition, $B_{W.u.}(M1; 3/2^+ \rightarrow 5/2^+) \simeq 3.1 \times 10^{-2}$ (see Table I in [35]), and the internal conversion coefficient $\alpha_{M1} \simeq 1.5 \times 10^9$ (the result of calculation by the computer code [36] for the transition energy of 8 eV)], \mathcal{E}_{res} is the electron resonance energy can be evaluated

as $\mathcal{E}_{\text{res}} = E_{\text{is}} - |\mathcal{E}_f| \simeq 1$ eV, since for 7s-electrons the binding energy in thorium atom equals $\mathcal{E}_f = 6.3$ eV [37], parameter $\lambda_e^{\text{res}} = 2\pi\hbar/\sqrt{2m\mathcal{E}_{\text{res}}}$ corresponds to the resonance de Broglie wavelength, n_e is the electron density in plasma, and τ is the plasma's life time which equals to the duration of the laser pulse $\tau_L \approx 15$ ns (see below).

The number of the ^{229}Th nuclei evaporated by a laser pulse from the target is

$$N_{229}^{\text{evap}} \simeq \frac{\beta \rho_{\text{ThO}_2} V}{[(1-\beta)(232+32) + \beta(229+32)]u} \simeq 2 \times 10^{13}, \quad (5)$$

where $\rho_{\text{ThO}_2} = 10$ g cm $^{-3}$ is the density of the thorium target, $u = 1.66 \times 10^{-24}$ g is the atomic mass unit. Here $V = \pi w_L^2 h$ is the laser plasma volume with the laser spot waist of $w_L = 5 \times 10^{-3}$ cm, and typical penetration depth of laser radiation of $h \simeq 10^{-4}$ cm. The latter is defined by the wavelength of excitation laser (1.06×10^{-4} cm). Parameter $\beta = 0.068$ stands for the fraction of ^{229}Th isotope in the target. In our experiments we used target containing 6.8% of the ^{229}Th nuclei with the rest of ^{232}Th nuclei (93.2%).

After evaporation of the target, the plasma expands. The front of the shock wave, which contains approximately of 10% of the evaporated ^{229}Th nuclei $N_{229} \simeq 0.1N_{229}^{\text{evap}}$, has a number density of thorium ions of $\simeq 10^{20}$ cm $^{-3}$ and a number density of electrons $n_e \simeq 10^{20}$ cm $^{-3}$ (the plasma is neutral as a whole). The front of the wave moves with the speed of sound absorbing laser radiation for a time τ_L and warming up to the electronic temperature of $kT \simeq 10$ eV.

Thus, for Maxwellian electron energy distribution $f_e(\mathcal{E})$ the excitation probability per one nucleus of ^{229}Th can be evaluated from Eq. (3). The result is

$$\eta_{\text{IC}} \simeq 10^{-5}. \quad (6)$$

Finally, we can evaluate the number of excited nuclei per laser pulse as

$$N_{\text{is}} \simeq \eta_{\text{IC}} N_{229} \simeq 10^8,$$

which sounds promising for further analysis. Besides excitation of ^{229}Th nuclei in laser ablation, this method allows to implant ionized thorium into a wide bandgap dielectric matrix and analyse them *in situ*.

III. ION IMPLANTATION INTO SiO_2 MATRIX

Previous studies of laser implantation of ^{232}Th ions in SiO_2 matrix [38] showed that a wide band dielectric compound $^{232}\text{Th}:\text{SiO}_2$ is formed in the subsurface area. Dependency of the band gap on Th/Si atomic fraction is shown in Fig. 2. The large band gap of at least 8 eV [5] is necessary to prevent prompt IC process of excited ^{229}Th nuclei. In this case (marked with gray color) one can expect that implanted excited isomeric ^{229}Th nuclei will slowly decay via γ channel. To reach this regime, the atomic ratio Th/Si should be less than 0.4.

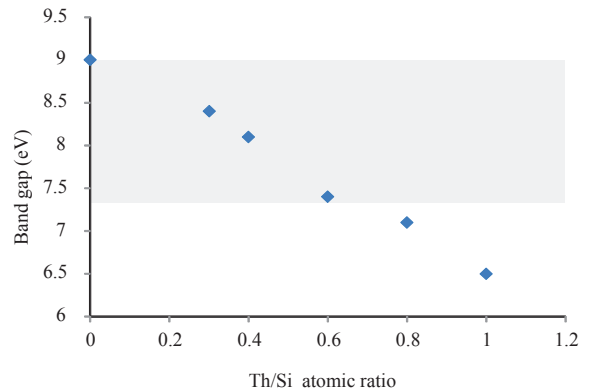


Figure 2: Dependency of the $^{232}\text{Th}:\text{SiO}_2$ compound band gap on relative number of thorium atoms according to surface chemical composition analysis using XPS and REELS methods [38].

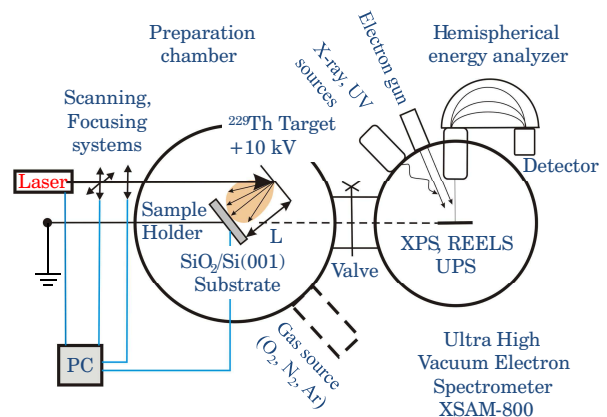


Figure 3: Experimental setup for target preparation and *in situ* analysis based on electron spectrometer XSAM-800 Kratos. 1 — sample loading and target preparation chamber, 2 — YAG:Nd laser for target ablation, 3 — precision manipulator 4 — valve, 5 — analysis chamber, 6 — hemispherical electron analyzer chamber equipped by X-ray and UV sources, and e-gun.

To provide this condition and to prepare the sample, we use method depicted in Fig. 3. The experimental setup bases on the XSAM-800 (Kratos, UK) electron spectrometer with the sample loading chamber upgraded for ablation and implantation of Th ions. The method allows to study different samples *in situ* in the ultra high vacuum (UHV) surface analysis system. Implantation of Th ions in SiO_2/Si target was performed directly in the spectrometer's preparation chamber. For laser ablation we use a target of thorium oxide (thin disk of 3 mm in diameter) deposited on 10 mm \times 10 mm silicon substrate. The overall activity of the ^{229}Th isotope in the target is around 100 kBq which is equivalent to 10^{16} nuclei. The main source of radioactivity are ^{229}Th nuclei which pro-

vide 99.988% of all α emitters in the target. Another source are ^{228}Th nuclei, which contribute by approximately 0.011%. The isotope ratio of ^{229}Th in the target equals 6.8%, the rest are ^{232}Th nuclei.

Focused radiation of a solid state Nd:YAG laser at $\lambda = 1064\text{nm}$ wavelength is used for target ablation. The laser operates in the Q-switched regime with the pulse energy of 100 mJ and pulse duration of 15 ns which provides power density I on a target in the range $10^9 - 10^{10}\text{ W/cm}^2$. Laser power density is the most critical parameter defining excitation probability η_{IC} . It determines electron temperature, degree of ionization, particle number density which enter the expression for η_{IC} (2). The laser focus was scanned on a target using deflection prisms controlled by a personal computer (PC). The amount of sputtered material could be varied by changing power density and the number of laser pulses. Ion component of laser plasma was accelerated in an electrical field between the target and SiO_2/Si substrate placed parallel to the target. Before the laser shot, the target has a potential of +10kV and is connected to the grounded substrate by 25 nF capacitor. During the laser shot, the capacitor discharges through plasma, while ions are accelerated and hit the substrate with energies of 10keV which is enough to implant in SiO_2 dielectric. The charge accumulated in the capacitor before the laser shot was adjusted to the expected net charge of the ion component in plasma (typically $\sim 10^{12} - 10^{13}$ ions per shot with the degree of ionization $\simeq 50\%$).

The target and the sample are separated by the distance of $L = 5\text{ cm}$. We evaluate the time-of-flight of thorium ion between the target and the sample as $< 10^{-7}\text{ s}$. It means, that independently of ion charge multiplicity, excited nuclei reach the target before decay via IC or other channels (see below). The large band gap of SiO_2 will block IC process immediately after implantation.

For sample preparation we typically use 5 laser pulses with the repetition rate of 0.2 Hz. Then the Th: SiO_2/Si sample was moved under UHV conditions from the preparation chamber into the analysis chamber using a mechanical tool. The transportation time from one chamber to another chamber is less than 30 s. In most experiments we use 6.5 nm SiO_2 film on Si(001) crystal, p -type 0.05 Ohm cm. Such thickness provides optimal sensitivity for photoelectron spectroscopy method which is described in the next Section. Concentration of thorium in the SiO_2 film was measured by X-ray photoelectron spectroscopy (XPS) with $\text{Al } K_\alpha$ emission at 1486.6 eV. Fractional number density of implanted Th nuclei is less than 1% which, according to fig. 2, corresponds to the Th: SiO_2 band gap of 9.0 eV. The band gap was measured by reflected electron energy loss spectroscopy (REELS).

IV. ELECTRON SPECTROSCOPY

We study $^{229}\text{Th}:\text{SiO}_2/\text{Si}$ sample using the sensitive XSAM-800 electron spectrometer (Fig. 3). We expect,

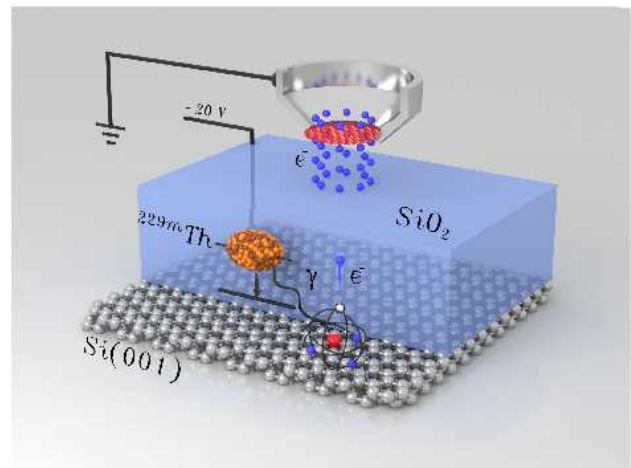


Figure 4: Decay of an excited ^{229}Th nucleus followed by emission of photoelectron from Si substrate. After penetration through 6.5 nm SiO_2 film photoelectrons are collected by XSAM- 800 electron spectrometer.

that VUV photons emitted in γ decay of excited ^{229}Th nuclei interact with Si substrate which plays a role of a photocathode. If SiO_2 layer is thin enough, photoelectrons can leave the sample and reach the spectrometer. The process is schematically shown in Fig. 4.

Thickness of silicon oxide used in experiments is determined, from one side, by implantation depth of thorium ions (typically 10 nm) and, from the other side, by extinction of electron signal in the SiO_2 layer. In most of experiments we used 6.5 nm thick SiO_2 film which suppresses electron signal by approximately 6 times for a normal incidence electron. To prevent cut-off close to zero photoelectron kinetic energies the accelerating potential of -20.0 V relative to the entrance aperture of the spectrometer is applied. Thus, the sample itself plays a role of an efficient photo cathode converting γ -quanta to low energy electrons. Compared to direct registration of γ -quanta (VUV photons) this approach provides much higher sensitivity.

Fig. 5 shows a sequence of electron energy spectra measured after different time intervals counted from the measurement start. For clarity, the spectra are shifted by 20.0 eV corresponding to potential difference between the sample and the spectrometer's aperture. Strong signal (up to $3000\text{ counts s}^{-1}$) is observed in the energy interval from 0 eV to 3 eV. The signal decreases in time and vanishes in several hours. Note, that after long time interval (e.g. 16 hours) the spectrum transforms in a background of approximately 15 eV width and integrated count rate of $\simeq 7\text{ s}^{-1}$ (see the inset in Fig. 5). Knowing the intensity of the background signal and half-life of the radionuclide, one can evaluate the total number of implanted ^{229}Th nuclei as 3×10^{12} . Within measurement uncertainty this coincides with estimate of thorium atomic concentration from XPS measurements.

We performed a set of experiments with different ab-

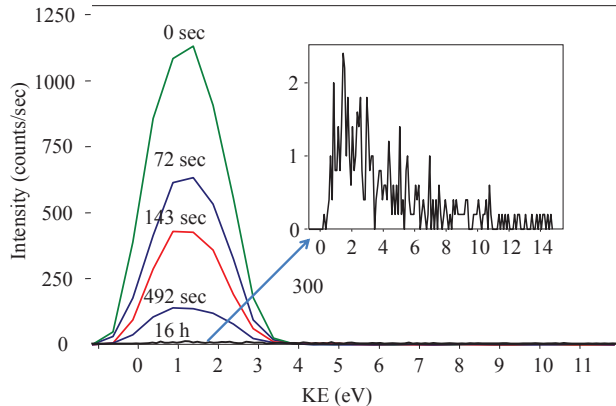


Figure 5: A sequence of electron energy spectra measured after different time intervals from the measurement start (shown on the plot). The inset shows the spectrum measured in 16 hours after implantation (magnified). Horizontal axis is corrected for the 20.0 eV offset corresponding to potential difference between the sample and the spectrometer’s aperture (Fig. 4). KE is photoelectron kinetic energy.

lated targets to study origin of the narrow-line signal shown in Fig. 5. Although there are no known long-living electronic states in silicon or silicon oxide which can be excited during ion implantation, we did experiments with pure silicon, pure carbon and some other targets for laser ablation (for more details see Section VII (Appendix)). After ablation, the procedure of sample preparation and analysis described in the Section III was reproduced. In these experiments we did not detect any signal in the expected energy range (0–3 eV). This observation confirms the absence of long-living electronic states in the sample. Even more stringent test was done with targets of isotopically pure ^{232}Th and ^{232}Th oxide film. We also did not see any signal similar to the one shown in Fig. 5, independently on the laser power density I . It proves that the origin of the signal comes purely from ^{229}Th atoms and we ascribe this peculiar signal to the process depicted in Fig. 4. We should note, that the signal amplitude is very sensitive to the laser power density I , which also confirms that the signal results from ICC process described in the Section II. Verification of results is described in more details in Section VII (Appendix).

V. THE NUCLEAR TRANSITION ENERGY FROM CALIBRATED ELECTRON SPECTRA

Good reproducibility and strong signal from $^{229}\text{Th}:\text{SiO}_2/\text{Si}$ sample allows to accurately measure dynamics of the process. Figure 6 shows time dependency of normalized signal obtained in three independent experiment series (in a logarithmic scale). The broad background coming from α -decay of ^{229}Th nuclei (the

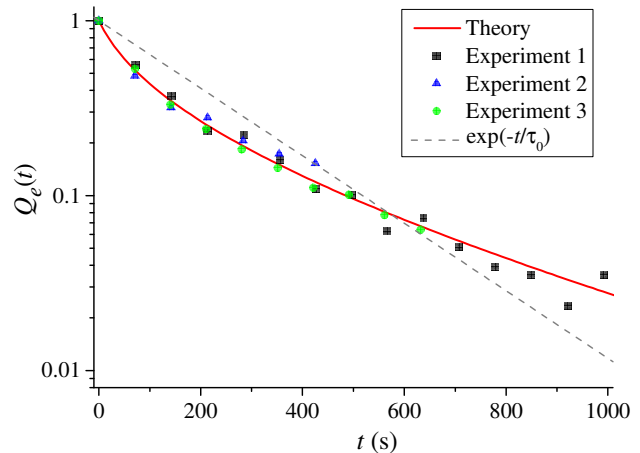


Figure 6: Time dependency of normalized experimental signal (dots) from three independent series of measurements. Dashed line — exponential decay with the constant $\tau_0 = 225$ s, red line — theoretical model from equation (12) for energy $E_{\text{is}} = 7.1$ eV and $T_{1/2} = 1880$ s.

inset in Fig. 5) is subtracted from the spectra before evaluation the data for Fig. 6. The decay deviates from exponential which can be interpreted as the Purcell effect (change of decay probability due to environment [39]) which is described in details in the Section VI.

To recover the energy of VUV photons emitted during decay of isomeric nuclei from photo electron spectra, we performed high resolution measurements. To achieve the uncertainty of 0.1 eV the spectra with high count rate of several thousand of electrons per energy bin are demanded, which requires long acquisition time of a few minutes. High-resolution spectrum measured during 500s is presented in Fig. 7, line 1. Reduction of the signal during the measurement results in distortion of the spectrum. We corrected the measured spectra according to the decay curve of Fig. 6 and then subtract the background coming from α -decay of ^{229}Th nuclei (the inset in Fig. 5). The corrected spectrum is shown in Fig. 7, line 2.

The energy $\hbar\omega_N$ of the emitted γ -quantum during isomeric transition in the ^{229}Th nucleus can be derived from usual equation of the photoeffect:

$$KE = \hbar\omega_N - BE - eU.$$

Here KE is the kinetic energy of electrons emitted from the silicon substrate (measured value), BE is the electron binding energy relatively to the vacuum energy level (E_{vac}), U is the potential difference between the sample and the detector. The latter is equal to the difference between the work function of the sample and that of the detector ($eU = WF_{\text{d}} - WF_{\text{Si}}$). In the case when $WF_{\text{Si}} < WF_{\text{d}}$, a part of the spectrum with electron energies close to zero is lost. To prevent this effect in our measurements, a negative potential $U_0 = -20.0$ V is applied to the sample, which gives $eU = eU_0 + WF_{\text{d}} - WF_{\text{Si}}$. This equation consists the term WF_{d} which value differs

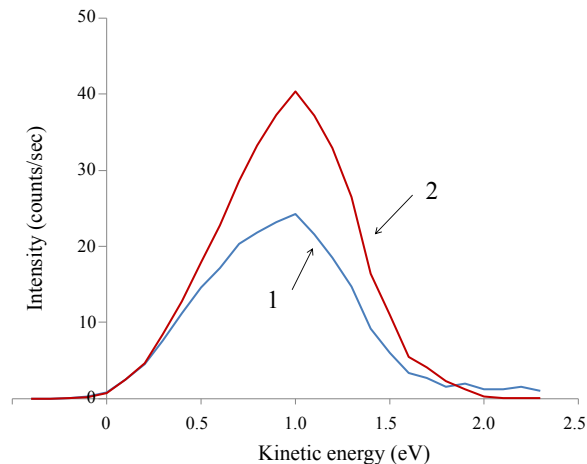


Figure 7: High resolution photo electron spectrum from $^{229}\text{Th}:\text{SiO}_2$ target measured during 500 s (line 1). The spectrum shape is corrected according to the decay curve of Fig. 6, then the background coming from α -decay of ^{229}Th is subtracted. Line 2 shows the corrected spectrum. Calibration of the energy scale was carried out using $\text{Si}2p$ line from silicon substrate obtained during XPS measurements (AlK α X-ray source was used).

for different devices and experimental conditions. In order to determine it one can use calibration of the energy scale of the analyzer using core levels of a reference material, obtained during XPS measurements. In our case, AlK α emission line with energy 1486.6 eV was used and a silicon was chosen to be a reference material as far as it's core lines are defined well. At first, such calibration allows one to shift the kinetic energy scale by choosing the WF_d value in order to make the position of spectral lines corresponded the KE values counted from the vacuum level of silicon substrate [40]. Secondly, it allows one to obtain the precision of kinetic energy determination about ± 0.05 eV over the whole energy scale due to the narrowness of XPS core lines [41].

XPS spectra of the sample under study after Th implantation is presented in Fig. 8. The energy difference between the $\text{Si}2p$ core level and the Si valence band maximum (VBM) reported in the literature is 98.80 eV [42]. Thus, the $\text{Si}2p$ binding energy relatively to the vacuum level for pure silicon substrate must be $BE_{\text{Si}2p} = 98.8 + 5.1 = 103.9$ eV. Converting this value to the values for kinetic energies of photoelectrons, knocking out from the level by X-ray AlK α radiation one can obtain the value $KE_{\text{Si}2p} = 1486.6 - 103.9 = 1382.7$ eV. The position of the $\text{Si}2p$ spectral line corresponding to the signal from silicon substrate in Fig. 8 is connected to that value. The use of such energy scale calibration independently on the applied voltage between the sample and the spectrometer allows one to count the KE value from the vacuum level of silicon substrate. This calibration was applied to the energy scale in Fig. 7 thus the right part of the spectrum with maximal value of kinetic

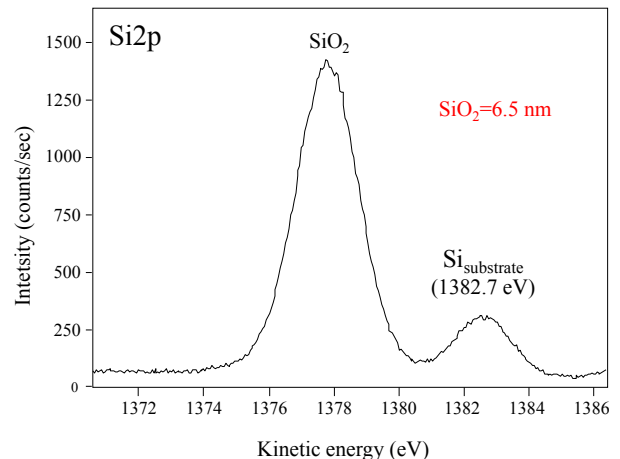


Figure 8: Calibration XPS spectra of $\text{Si}2p$ lines for the sample $\text{Th}:\text{SiO}_2/\text{Si}$ formed after Th implantation.

energy (KE_{max}) would correspond to the energy of photoelectrons from the edge of the Si valence band:

$$KE_{\text{max}} = \hbar\omega_N - WF_{\text{Si}}. \quad (7)$$

The left edge of the spectrum (KE_{min}) corresponds to photoelectrons which leave the surface at energies close to zero. They can be not only primary low-energy electrons which are directly exited from a filled state with an energy below E_{vac} , but also higher energy electrons scattered on their way toward the surface. These electrons define the cutoff of a photoelectron spectrum and define the zero of the energy scale for the case of clean silicon. However, in our case there is a dielectric SiO_2 layer on Si substrate, which means that the measured KE_{min} should be equal to the potential difference between SiO_2 surface end detector. Due to the presence of a dipole at SiO_2/Si interface, the potential of the SiO_2 surface is different from the one of Si. It means, that the photoelectron spectrum coming from the Si substrate can change significantly in the cutoff energy region after passing through the energy barrier at the interface.

In order to determine $\hbar\omega_N$ it is necessary to determine the absolute KE_{max} value after the above mentioned spectrum energy scale calibration procedure. However, the shape of the electron spectrum caused by UV sample irradiation has a complex structure. In the easiest model if not taken into account the energy dependence of such important physical parameters like density of electronic states, photoionization cross-section of valence electrons, the values of matrix elements of electron transitions between sublevels of the valence band and conductance band, the spectrum is mainly determined by the processes of elastic and inelastic scattering.

Really, according to Ref. 43 the main part of photoelectrons, before leaving the sample encounter several acts of inelastic collisions, as a result of which the initial photoelectron lose part of it's initial energy. It leads to the fact

that a part of a spectrum formed by electrons with maximal energy is redistributed to the spectrum energy range corresponding to low electron kinetic energies. Thus the main point is shifted to the minimal kinetic energy. At the same time, the right edge of the spectrum has a monotonically damped character and there can be no sharp edge of the spectrum observed usually for metals while irradiating by UV of 20 or 40 eV or X-ray. The modeling of the spectral line shape in our case is a complex task, that requires determination of many parameters, including the ones related to device. In order to avoid labour-intensive and probably non correct model calculations within the framework of this work we use a simple empirical method that is based in the comparison of the right edge of the photoelectron spectra obtained for the studied samples and VUV sources with known spectral characteristics.

We used UV source (Xe discharge lamps) for modeling photoionization from Th:SiO₂/Si. The photon energy of this lamp is close to the expected spectral line coming from the ²²⁹Th isomeric state decay (see Table I). The emission spectra of this lamp (see Fig. 9) together with corresponding photoelectron spectra from decay Th:SiO₂/Si are analyzed in details. Using results of our analysis, we agreed of the following procedure for preparation of photoelectron spectra:

- after implantation, we recorded photoelectron spectra from ²²⁹Th:SiO₂/Si sample in high resolution mode. The sample substrate is at $U_0 = -20.0$ V potential corresponding to the spectrometer aperture. The spectra intensity are corrected according to procedure described in Fig. 7;
- using the same high resolution mode and the same U_0 applied to the sample we recorded photoelectron spectra from ²²⁹Th:SiO₂/Si sample under illumination by Xe VUV lamp and under X-Ray source AlK α (1486.6 eV);
- for all spectra we use the same calibration of the energy scale, namely, shift of the scale to the position of the Si2p line, which is obtained using the X-Ray source AlK α at $KE_{Si2p}=1382.7$ eV;
- the analysis of the spectrum of sample irradiated with Xe VUV lamp showed that the right values of KE_{max} is obtained when using the extrapolation with linear function tangent to the high-energy

Table I: Spectral lines of xenon discharge lamp and corresponding KE_{max} energies for the photoelectron spectra presented in Fig. 10. The last row shows deduced KE_{max} energy for ²²⁹Th:SiO₂/Si sample with decaying isomeric ²²⁹Th nuclei.

UV Source	λ (nm)	$\hbar\omega$ (eV)	$KE_{max} = \hbar\omega - WF_{Si}$ (eV)
Xe	147	8.4	$3.3^{(+0.1)}_{(-0.2)}$
Th:SiO ₂ /Si		$7.1^{(+0.1)}_{(-0.2)}$	$2.0^{(+0.1)}_{(-0.2)}$

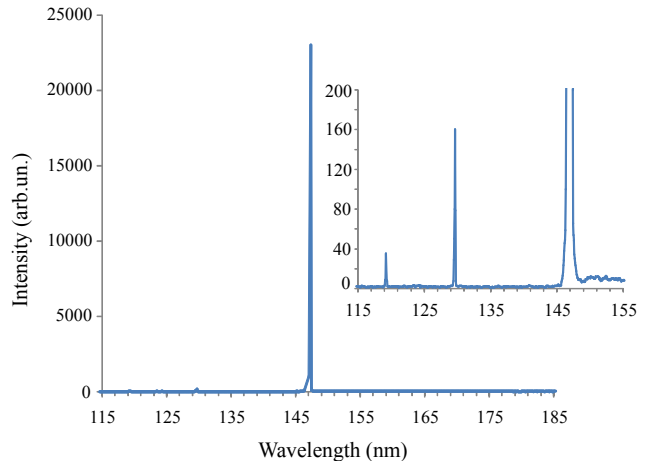


Figure 9: VUV spectra of xenon (Xe) discharge lamp manufactured by CHROMDET Ltd. (Russian Federation).

shoulder of the spectrum in the range of spectrum intensity from 5% to 1% and finding the intersection with x-axis as shown in Fig. 10. The accuracy of determining KE_{max} by this method has asymmetry character and better than $-0.2/+0.1$ eV;

- the same method definition of KE_{max} we use for spectrum, obtained for ²²⁹Th:SiO₂/Si sample during decay (Fig. 10).

Fig. 10 shows high resolution photoelectron spectra from ²²⁹Th:SiO₂/Si sample irradiated by VUV lamp and during isomeric decay after intensity normalization and energy calibration. Using the same method of tangent line we derive that the maximum kinetic energy of photoelectrons KE_{max} excited in silicon by photons during ²²⁹Th isomeric state decay in Th:SiO₂/Si structure is $2.0^{(+0.1)}_{(-0.2)}$ eV. The uncertainty comes from combined fit and extrapolation uncertainties of KE_{max} and the energy calibration uncertainty of the electron spectrometer according to its specification. Results are summarized in Table I.

Thus, using the value $KE_{max} = 2.0^{(+0.1)}_{(-0.2)}$ eV for ²²⁹Th:SiO₂/Si sample with decaying isomeric ²²⁹Th nuclei, we substitute it in the equation $\hbar\omega_N = 5.1 + KE_{max}$, and obtain the nuclear transition energy of:

$$E_{is} = \hbar\omega_N = 7.1^{(+0.1)}_{(-0.2)} \text{ eV.}$$

Comparing to the known value of 7.8 ± 0.5 eV obtained in experiments with a cascade decays [4, 5], our result is 3 times more accurate and deviates by 1.5 joint standard deviations. Further decrease of uncertainty is possible by direct optical spectroscopy of VUV photons emitted by isomeric ²²⁹Th nuclei implanted in the dielectric sample. To overcome the problem of weak photon signal one can increase the number of implanted ²²⁹Th by several orders of magnitude, since the suggested excitation-implantation method is easily scalable.

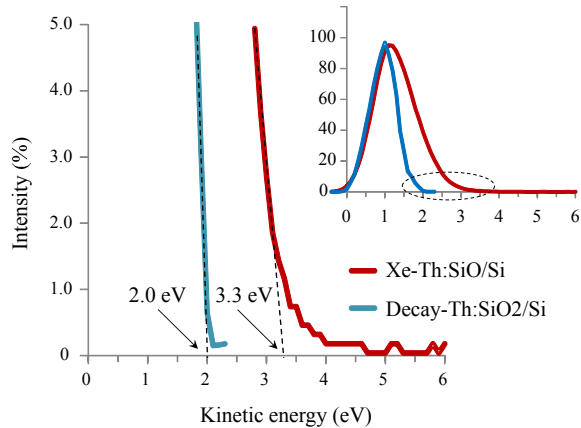


Figure 10: Normalized photoelectron spectra from $^{229}\text{Th}:\text{SiO}_2/\text{Si}$ sample after illumination by VUV radiation of xenon (Xe) discharge lamps. The same plot shows the photoelectron spectrum from $^{229}\text{Th}:\text{SiO}_2/\text{Si}$ sample during isomeric decay. Maximal electron energy KE_{max} for each spectrum is derived from extrapolation of the linear function tangent to the right wing of the spectrum to the x-axis.

VI. THE ISOMERIC LEVEL HALF-LIFE AND REDUCED PROBABILITY OF THE NUCLEAR TRANSITION

The isomeric nuclei decay in $^{229}\text{Th}:\text{SiO}_2/\text{Si}$ sample shows a pronounced non-exponential behaviour (Fig. 6) which can be explained by physical and chemical environment [44]. Indeed, the isomeric nuclear decay rate depends on (i) refractive index surrounding medium [9, 10] and (ii) presence of vacuum/ SiO_2 and $\text{SiO}_2/\text{Si}(001)$ interfaces which cause so-called Purcell effect [39]. The decay probability in presence of interfaces is different from the one in infinite medium by the Purcell factor.

The theory of Purcell effect for the case similar to ours is discussed in [45, 46] for the atomic $E1$ transition. We generalized their approach for the case of $M1$ transitions. The formulas for the $M1$ Purcell factors have the following form [44]:

$$f_P(z) = f_P^r(z) + f_P^{nr}(z), \quad (8)$$

where

$$f_P^r(z) = \int_0^1 \mathcal{F}(z, \kappa) d\kappa, \quad f_P^{nr}(z) = \int_1^\infty \mathcal{F}(z, \kappa) d\kappa, \quad (9)$$

are respectively the radiative and nonradiative decay-rate constants (see below), κ is the reduced transverse momentum of the photon $\kappa = \sqrt{k_{1x}^2 + k_{1y}^2}/k_1$, where $k_1 = \sqrt{\varepsilon_1}\omega_N/c$, and ε_1 is the dielectric constant of the

SiO_2 film. Function $\mathcal{F}(z, \kappa)$ in Eq. (9) is defined as

$$\begin{aligned} \mathcal{F}(z, \kappa) = & \frac{1}{2} \text{Im} \left\{ \frac{F(\hat{d}_0 - \hat{z}, R_{12}^\perp) F(\hat{z}, R_{13}^\perp) \kappa^3}{F(\hat{d}_0, -R_{12}^\perp R_{13}^\perp) l_1} \right. \\ & + \left[(1 - \kappa^2) \frac{F(\hat{d}_0 - \hat{z}, -R_{12}^\perp) F(\hat{z}, -R_{13}^\perp)}{F(\hat{d}_0, -R_{12}^\perp R_{13}^\perp)} \right. \\ & \left. \left. + \frac{F(\hat{d}_0 - \hat{z}, -R_{12}^\parallel) F(\hat{z}, -R_{13}^\parallel)}{F(\hat{d}_0, -R_{12}^\parallel R_{13}^\parallel)} \right] \frac{\kappa}{l_1} \right\}. \quad (10) \end{aligned}$$

Here $F(x, y) = 1 + y \exp(-2l_1 x)$, $\hat{d}_0 = k_1 d_0$, $\hat{z} = k_1 z$ with d_0 being the thickness of the SiO_2 film ($d_0 = 6.5$ nm in our case). The distance z is counted from the certain ^{229}Th nucleus and the vacuum/ SiO_2 interface (accordingly, $d_0 - z$ is the distance between the ^{229}Th nucleus and the SiO_2/Si interface). The reflection coefficients in Eq. (8) are defined as

$$R_{1,j}^\parallel = \frac{\varepsilon_1 l_j - \varepsilon_j l_1}{\varepsilon_1 l_j + \varepsilon_j l_1}, \quad R_{1,j}^\perp = \frac{\varepsilon_1 - \varepsilon_j}{\varepsilon_1 + \varepsilon_j}, \quad (11)$$

where $j = 2, 3$, and $l_j = -i\sqrt{\varepsilon_j/\varepsilon_1 - \kappa^2}$ (we remained notations from [45, 46]). In Eqs. (8)–(11), $l_1 = -i\sqrt{1 - \kappa^2}$.

In Eq. (9), the function $f_P^r(z)$ gives the radiative decay-rate constant for energy transfer to the vacuum through the vacuum/ SiO_2 interface [46]. Correspondingly, the number of emitted photons is proportional to the function f_P^r . The function $f_P^{nr}(z)$ gives the nonradiative decay-rate constant for energy transfer into the Si substrate [46]. This component exists since the imaginary part of the Si dielectric constant is different from zero. The number of photoelectrons is proportional to the energy absorbed in the Si substrate, i.e. to the function f_P^{nr} .

The Purcell factor depends on the position of the emitting object relative to interfaces. In order to calculate the functions $f_P(z)$, $f_P^r(z)$, and $f_P^{nr}(z)$ numerically, we divided thin SiO_2 film in 0.1 nm thick layers. For each layer at the distance of z_i from the vacuum interface, the Purcell factor was calculated for the following values of dielectric constants: $\sqrt{\varepsilon_1} = 1.75$ (measured in this work), $\sqrt{\varepsilon_2} = 0.7 + i2.4$ for Si at the photons energy 7.1 eV [47], and $\sqrt{\varepsilon_3} = 1$ for vacuum. The result of the calculation is shown in Fig. 11.

In our experiment, we detect not photons, but photoelectrons from Si substrate coming from isomeric ^{229}Th nuclei decay in thin SiO_2 film. The photoelectron signal detected by the spectrometer (Fig. 6) is simulated by the following function:

$$Q_e(t) = \frac{1}{N} \sum_i \lambda_{\text{nr}}(z_i) e^{-z_i/z_0} e^{-\lambda(z_i)t}, \quad (12)$$

where N is the normalization providing $Q_e(0) = 1$. Distribution of ^{229}Th nuclei in SiO_2 along z axis is described by the exponential function e^{-z_i/z_0} with $z_0 = 6$ nm [38].

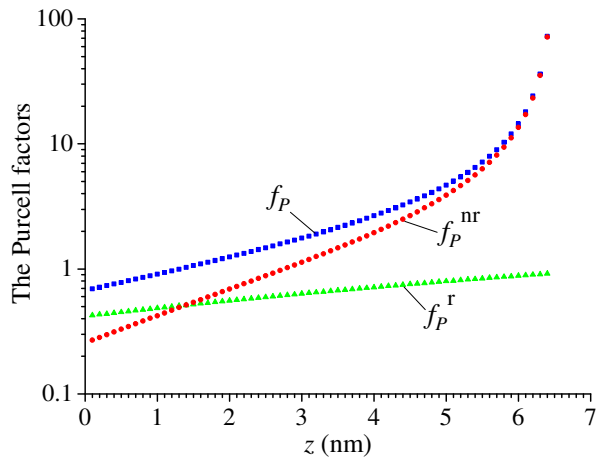


Figure 11: The total, f_P , radiative, $f_P^r(z)$, and nonradiative, $f_P^{nr}(z)$, Purcell factors calculated from Eqs. (8–10) for the M1 isomeric transition in our $^{229}\text{Th}:\text{SiO}_2/\text{Si}$ sample for nuclei placed at the distance z from the vacuum interface.

The decay constants $\lambda(z_i)$ and $\lambda_{nr}(z_i)$ in i -th layer of the SiO_2 film are given by

$$\begin{aligned}\lambda(z_i) &= f_P(z_i)n_{\text{SiO}_2}^3 \ln(2)/T_{1/2}, \\ \lambda_{nr}(z_i) &= f_P^{nr}(z_i)n_{\text{SiO}_2}^3 \ln(2)/T_{1/2},\end{aligned}$$

where $T_{1/2}$ is the isomeric state half-life of the bare nuclei in vacuum, $n_{\text{SiO}_2} = \sqrt{\varepsilon_1}$.

Thus, the non-exponential behaviour of the signal shown in Fig. 6 can be explained by the fact that isomeric nuclei implanted close to the SiO_2/Si interface have much faster decay (more than by one order of magnitude) compared to nuclei sitting close to the Si/vacuum interface. Since the number density of isomeric nuclei change only by approximately factor of e from one interface to another, the z -dependent Purcell factor significantly changes dynamics of our signal. It is also interesting to note that the simultaneous measurement of photons and electrons would give different decay curves.

We approximate experimental data from Fig. 6 by $Q_e(t)$ using only one fit parameter $T_{1/2}$. The result is

$$T_{1/2} = 1880 \pm 170 \text{ s} \quad (13)$$

which corresponds to the half life of the bare isomeric ^{229}Th nucleus in vacuum. One can mention very good correspondence between experimentally measured and calculated dynamics of the signal which confirms our model for interaction between excited nuclei and environment.

From the half-life $T_{1/2}$ one can derive the reduced probability of the nuclear magnetic-dipole transition from the excited state with the spin $3/2^+$ to the ground state with the spin $5/2^+$:

$$B_{W.u.}(M1; 3/2^+ \rightarrow 5/2^+) = (3.3 \pm 0.3) \times 10^{-2}. \quad (14)$$

This value is close to the average value of 3.1×10^{-2} obtained in [35] (see Table I) in the frame of the rotational model.

VII. APPENDIX I: EXPERIMENTS WITH OTHER TARGETS. CROSS-CHECKS AND DISCUSSION

We made a set of dedicated experiments aimed to check results of Section IV. Although there are no known long-living electronic states in silicon or silicon oxide which can cause electron emission similar to one shown in Fig. 5, it is obligatory to demonstrate that the signal is caused purely by excited ^{229}Th isotope nuclei. We made a number of experiments with test targets not containing ^{229}Th isotope. The targets of (i) metallic ^{232}Th (isotopically pure), (ii) ^{232}Th (isotopically pure) oxide, (iii) graphite, (iv) silicon and (v) thin silicon oxide film on silicon were laser ablated and then the regular experimental procedure described in Section IV was carried out. None of these experiments resulted in any spectral feature similar to the very peculiar electronic spectra appearing after implantation of ^{229}Th isotope (Fig. 5).

As a quantitative check we evaluated the expected electron count rate assuming that it is caused by decay of ^{229}Th nuclear isomeric state.

Taking into account expected losses of electrons in our experimental configuration and knowing the count rate directly after implantation ($I_{SE} \approx 3000 \text{ s}^{-1}$) the number of excited nuclei in the sample can be estimated from the relation

$$N_{\text{is}} = \frac{T_{1/2}}{n_{\text{SiO}_2}^3} \frac{I_{SE}}{QE_{\text{Si}} \times CE \times LS} \approx 10^8,$$

where $QE_{\text{Si}} \approx 0.3$ is the quantum efficiency of silicon in VUV range, $CE \approx 0.5$ is the acceptance efficiency of XSAM-800 spectrometer, $LS \approx 0.17$ is extinction coefficient of photoelectrons in 6.5 nm silicon oxide film (measured with XPS).

Knowing N_{is} , one can evaluate the excitation probability of ^{229}Th isomeric nuclear state in ICC process. Taking into account that the net number of ^{229}Th nuclei in the sample is $N_{229} \approx 3 \times 10^{12}$, the excitation probability is on the order $N_{\text{is}}/N_{229} \sim 10^{-5}$. This value is of the same order as theoretical expectation from equation (3) evaluated for optimal plasma conditions ($\eta_{\text{IIC}} \simeq 10^{-5}$, Eq. (6)).

As follows from Maxwellian distribution, the excitation probability η_{IIC} depends exponentially on the electron plasma temperature. Thus, the decrease of electron plasma temperature should result in a sharp decrease of IIC efficiency and, consequently, the excitation probability. We carried out a test experiment with decreased laser power density on the target while all other experimental conditions remain unchanged. In this experiment the illuminated area was increased by a factor of 4 at the same pulse energy which resulted in 4 times decrease of laser power density. Under this experimental conditions we did not see any signature of secondary electron emission which can be ascribed to decay of ^{229}Th isomeric nuclear state.

The test experiments clearly indicate that the electron signal is directly related with implanted ^{229}Th ions. Moreover, its amplitude is similar to one expected from ICC process in laser plasma at optimal parameters and is very sensitive to electron plasma temperature. We conclude, that the signal comes from decay of ^{229}Th low-lying isomeric state as depicted in Fig. 4. Of course, it would be highly desirable to measure the photon signal directly by optical methods, but the detection efficiency in current experimental configuration would be three orders of magnitude lower compared to electron signal which is close to the noise level coming from radioactive ^{229}Th isotope. It should be mentioned, that our experimental method upgraded with a dedicated optical registration setup may result in crucial increase of the accuracy for the transition energy. Even simple narrow-band filters or low-resolution spectrometer may improve the relative uncertainty to 10^{-3} level, while the high resolution setups allow to reach 10^{-5} relative uncertainty.

It should be noted that the electron spectra from $^{229}\text{Th}:\text{SiO}_2/\text{Si}$ sample were measured in the electron counting regime of XSAM-800 spectrometer. The photoelectron spectra from VUV light sources were measured

in the current measurement regime (saturation regime). Using one of the VUV sources we checked that the spectra measured in different regimes have fully identical shape.

VIII. ACKNOWLEDGMENTS

Authors are grateful the following colleagues for helpful discussions and experimental setup: V.I. Troyan, V.P. Yakovlev, K.Yu. Khabarova, A.V. Shutov, A.V. Zenkevich, Yu.N. Kolosov.

One of the authors (E.T.) is grateful colleagues from the University of California, Los Angeles Prof. E.R. Hudson, Dr. Ch. Schneider, and Dr. J. Jeet for helpful advice and constant readiness to help in the work.

This research was supported by a grant from the Russian Science Foundation (Grant No. 16-12-00001).

IX. REFERENCES

-
- [1] L. A. Kroger and C. W. Reich, Nucl. Phys. A **259**, 29 (1976).
- [2] C. W. Reich and R. G. Helmer, Phys. Rev. Lett. **64**, 271 (1990).
- [3] R. G. Helmer and C. W. Reich, Phys. Rev. C **49**, 1845 (1994).
- [4] B. R. Beck, J. A. Becker, P. Beiersdorfer, G. V. Brown, K. J. Moody, J. B. Wilhelmy, F. S. Porter, C. A. Kilbourne, and R. L. Kelley, Phys. Rev. Lett. **98**, 142501 (2007).
- [5] B. R. Beck, J. A. Becker, P. Beiersdorfer, G. V. Brown, K. J. Moody, J. B. Wilhelmy, F. S. Porter, C. A. Kilbourne and R. L. Kelley, Report LLNL-PROC-415170.
- [6] L. von der Wense, B. Seiferle, M. Laatiaoui, J. B. Neumayr, H. J. Maier, H. F. Wirth, C. Mokry, J. Runke, K. Eberhardt, C. E. Dullmann, et al., Nature **533**, 47 (2016).
- [7] V. F. Strizhov and E. V. Tkalya, Sov. Phys. JETP **72**, 387 (1991).
- [8] A. M. Dykhne, N. V. Eremin, and E. V. Tkalya, JETP Lett. **64**, 345 (1996).
- [9] E. V. Tkalya, JETP Lett. **71**, 311 (2000).
- [10] E. V. Tkalya, A. N. Zherikhin, and V. I. Zhudov, Phys. Rev. C **61**, 064308 (2000).
- [11] V. V. Flambaum, Phys. Rev. Lett. **97**, 092502 (2006).
- [12] E. V. Tkalya, Phys. Rev. Lett. **106**, 162501 (2011).
- [13] E. V. Tkalya and L. P. Yatsenko, Laser Phys. Lett. **10**, 105808 (2013).
- [14] E. Peik and C. Tamm, Europhys. Lett. **61**, 181 (2000).
- [15] G. A. Kazakov, A. N. Litvinov, V. I. Romanenko, L. P. Yatsenko, A. V. Romanenko, M. Schreitel, G. Winkler, and T. Schumm, New J. Phys. **14**, 083019 (2012).
- [16] E. Peik and M. Okhaphkin, C. R. Phys. **16**, 516 (2015).
- [17] C. J. Campbell, A. G. Radnaev, A. Kuzmich, V. A. Dzuba, V. V. Flambaum, and A. Derevianko, Phys. Rev. Lett. **108**, 120802 (2012).
- [18] P. V. Borisyuk, O. S. Vasilev, S. P. Derevyashkin, N. N. Kolachevsky, Y. Y. Lebedinskii, S. S. Poteshin, A. A. Sysoev, E. V. Tkalya, D. O. Tregubov, V. I. Troyan, et al., Quantum Electronics **47**, 406 (2017).
- [19] L. von der Wense, B. Seiferle, and P. G. Thirolf, Measurement Techniques **60**, 1178 (2018).
- [20] O. A. Herrera-Sancho, N. Nemitz, M. V. Okhaphkin, and E. Peik, Phys. Rev. A **88**, 012512 (2013).
- [21] O. A. Herrera-Sancho, M. V. Okhaphkin, K. Zimmermann, C. Tamm, E. Peik, A. V. Taichenachev, V. I. Yudin, and P. Glowacki, Phys. Rev. A **85**, 033402 (2012).
- [22] M. V. Okhaphkin, D. M. Meier, E. Peik, M. S. Safronova, M. G. Kozlov, and S. G. Porsev, Phys. Rev. A **92**, 020503(R) (2015).
- [23] A. Radnaev, C. Campbell, and A. Kuzmich, Phys. Rev. A **86**, 060501 (2012).
- [24] T. Takano, M. Takamoto, I. Ushijima, N. Ohmae, T. Akatsuka, A. Yamaguchi, Y. Kuroishi, H. Mune Kane, B. Miyahara, and H. Katori, Nature Photonics **10**, 662 (2016).
- [25] J. Jeet, C. Schneider, S. T. Sullivan, W. G. Rellergert, S. Mirzadeh, A. Cassanho, H. P. Jenssen, E. V. Tkalya, and E. R. Hudson, Phys. Rev. Lett. **114**, 253001 (2015).
- [26] S. Stellmer, G. Kazakov, M. Schreitel, H. Kaser, M. Kolbe, and T. Schumm, *On an attempt to optically excite the nuclear isomer in Th-229*, arXiv:1803.09294v1.
- [27] W. G. Rellergert, D. DeMille, R. R. Greco, M. P. Hehlen, J. R. Torgerson, and E. R. Hudson, Phys. Rev. Lett. **104**, 200802 (2010).
- [28] M. P. Hehlen, R. R. Greco, W. G. Rellergert, S. T. Sullivan, D. DeMille, R. A. Jackson, E. R. Hudson, and J. R. Torgerson, J. Luminescence **49**, 133 (2013).

- [29] P. Dessoovic, P. Mohn, R. Jackson, G. Winkler, M. Schreit, G. Kazakov, and T. Schumm, *J. Phys.: Condens. Matter* **26**, 105402 (2014).
- [30] S. Stellmer, M. Schreitl, and T. Schumm, *Sci. Rep.* **5**, 15580 (2015).
- [31] Sometimes this process is called as nuclear excitation by electronic capture (NEEC) (see for example C. J. Chiara *et al.* *Nature* **554**, 216 (2018) in and references therein). But in this paper, we will use the name given to the process by the authors [32] themselves, namely, the inverse internal conversion.
- [32] V. I. Goldanskii and V. A. Namiot, *Phys. Lett. B* **62**, 393 (1976).
- [33] E. V. Tkalya, *Laser Phys.* **14**, 360 (2004).
- [34] L. Torrisi, S. Gammino, A. Picciotto, D. Margarone, L. Laska, J. Krasa, K. Rohlena, and J. Wolowski, *Rev. Sci. Instrum.* **77**, 03B708 (2006).
- [35] E. V. Tkalya, C. Schneider, J. Jeet, and E. R. Hudson, *Phys. Rev. C* **92**, 054324 (2015).
- [36] I. M. Band and V. I. Fomichev, *At. Data Nucl. Data Tabl.* **23**, 295 (1979).
- [37] A. Kramida, Yu. Ralchenko, J. Reader, and NIST ASD Team, *NIST Atomic Spectra Database* (ver. 5.3), National Institute of Standards and Technology, Gaithersburg, MD, 2015. <http://physics.nist.gov/asd>.
- [38] P. V. Borisyuk, E. V. Chubunova, Y. Y. Lebedinskii, E. V. Tkalya, O. S. Vasilyev, V. P. Yakovlev, E. Strugovshchikov, D. Mamedov, A. Pishtshev, and S. Z. Karazhanov, *Laser Phys. Lett.* **15**, 056101 (2018).
- [39] E. M. Purcell, *Phys. Rev.* **69**, 681 (1946).
- [40] K. M. N. Fujimura, A. Ohta and S. Miyazaki, *Japanese Journal of Applied Physics* **55**, 08PC06 (2016).
- [41] D. Briggs and J. T. Grant, *Surface analysis by Auger and x-ray photoelectron spectroscopy* (IMPublications, Chichester, UK, 2003).
- [42] A. M. M. Perego and G. Seguini, *ApplPhysLett* **101**, 211606 (2012).
- [43] C. N. Berglund and W. E. Spicer, *Phys. Rev.* **136**, 1030 (1964).
- [44] E. V. Tkalya, *Phys. Rev. Lett.* **120**, 122501 (2018).
- [45] R. R. Chance, A. H. Miller, A. Prock, and R. Silbey, *J. Chem. Phys.* **63**, 1589 (1975).
- [46] R. R. Chance, A. Prock, and R. Silbey, *Adv. Chem. Phys.* **37**, 1 (1978).
- [47] S. Adachi, *Optical Constants of Crystalline and Amorphous Semiconductors. Numerical Data and Graphical Information* (Springer Science + Business Media, LLC, New York, 1999).